

# Formal Evolutionary Development of Low-Entropy Dendritic Thermal Systems

Marcelo H. Kobayashi\* and Hugo-Tiago C. Pedro<sup>†</sup>

*University of Hawaii at Manoa, Honolulu, Hawaii 96822*

Carlos F. M. Coimbra<sup>‡</sup>

*University of California, Merced, Merced, California 95344*

and

Alexandre K. da Silva<sup>§</sup>

*University of Texas at Austin, Austin, Texas 78712-0284*

DOI: 10.2514/1.42410

The present work contributes to the formal evolutionary development of complex thermal physical systems by using a bioinspired evolutionary method. The bioinspired method combines Lindenmayer systems with a turtle interpretation for the modeling of the complex dendritic structures, plus a finite element method for the analysis of the structure and an evolutionary algorithm to evolve the topology of the dendritic structure. With the proposed method, the optimal planar topology of a conductive dendritic structure for draining thermal energy from a fixed-area subject to uniform heat generation, a problem originally addressed by constructal theory, is investigated. The results show that the evolutionary approach can yield complex dendritic topologies that excel in performance and robustness. Moreover, our results demonstrate that a better performance in heat removal implies an increased complexity, up to an optimal level, of the draining system. Indeed, it is shown also that there is an optimal level of complexity beyond which the performance of the system is not substantially improved, which is in agreement with results reported in the literature. Finally, the robustness of hierarchical, dendritic complex topologies for heat transfer systems is discussed and quantified.

## Nomenclature

$A$	=	domain area
$k$	=	thermal conductivity
$L$	=	length scale
$n$	=	unit normal exterior-pointing vector
$Q$	=	heat source
$q'''$	=	heat source
$S$	=	entropy
$T$	=	temperature
$\varepsilon$	=	thermal conductivity ratio, $k_0/k_f$
$\xi$	=	dimensionless heat generation
$\Phi$	=	area ratio, $A_f/A$

## Subscripts

$f$	=	fin
$0$	=	root

## Superscript

*	=	nondimensional quantity
---	---	-------------------------

## I. Introduction

THE thermodynamic process of heat and mass transport from a source point to an area using a limited amount of material is encountered in a variety of natural and engineered systems, from cardiovascular and respiratory networks to the transport structure of plants and leaves and from heat and mass exchangers in thermal systems to circuits [1–9]. Although such systems vary in shape and structure, the efficiency of their designs can be generally measured by the reversibility of the cascading processes involved for obtaining the same output. For a given transport gradient, the higher the complexity of the system, the lower the entropy generated in each of the stages that make up the system. Thus, a complex internal combustion engine has a number of cascading processes that operate between the extreme temperature levels (e.g., between the adiabatic flame and the ambient temperatures). The higher the number of intermediate cascading processes involved, the higher the complexity of the system and the lower the entropy generated for a given energy potential available [9].

For engineered systems, incremental gains in efficiency are possible with the increased complexity or reversible stages, but these may result in large increments of complexity that are not currently commercially viable. Similarly, natural systems take advantage of threshold levels of complexity with cutoff scales beyond which any additional structure adds little to the overall performance [1–3,9]. In this work, the formal evolutionary process that naturally selects optimal levels of complexity for a simple transport problem is studied. The results show that there is a drive for complex structures until the point of diminishing returns limits the complexity of systems from developing into a runaway cascade of infinite smaller scales.

Dendritic structures and their inherent advantages in channeling flows of mass and energy in natural systems have been addressed in many previous studies [3,7,10–14]. Optimal geometrical features for a variety of applications have been identified as a result of such studies, with constructal theory being the most prominent method used in this area (e.g., [7]). Recently, a series of studies employed evolutionary processes similar to those observed in nature to propose a new generation of high-performance engineering devices [10–14].

Received 26 November 2008; accepted for publication 15 March 2009.  
Copyright © 2009 by Marcelo H. Kobayashi. Published by the American Institute of Aeronautics and Astronautics, Inc., with permission. Copies of this paper may be made for personal or internal use, on condition that the copier pay the \$10.00 per-copy fee to the Copyright Clearance Center, Inc., 222 Rosewood Drive, Danvers, MA 01923; include the code 0887-8722/09 and \$10.00 in correspondence with the CCC.

\*Associate Professor, Department of Mechanical Engineering, 2540 Dole Street, Holmes 301. Member AIAA (Corresponding Author).

<sup>†</sup>Research Assistant, Department of Mechanical Engineering, 2540 Dole Street, Holmes 301. Student Member AIAA.

<sup>‡</sup>Associate Professor, School of Engineering, P.O. Box 2039. Senior Member AIAA.

<sup>§</sup>Assistant Professor, Department of Mechanical Engineering, 1 University Station C2200. Member AIAA.

One of the key features of such designs is their hierarchical complexity. In other words, such systems have the ability to collect or deliver energy or mass to an area or volume in a nearly uniform and reversible way. The general problem of determining optimal dendritic structures for heat and mass transfer can also be cast as a topology optimization problem, for which many effective methods exist in the literature [15–18].

Taking account of the preceding, the main objective of the present work is to contribute to this line of research by quantifying the effectiveness and the robustness of added complexity of a family of trees through the use of a bioinspired evolutionary topology optimization algorithm. The concept proposed in this work is a new topology optimization method that is biologically inspired and that can evolve geometrical features on a genetic basis. Specifically, a method that uses Lindenmayer's L systems [19,20] in conjunction with its turtle interpretation [21,22] to model the graph topology of dendritic or tree-shaped structures is proposed. L systems were first proposed by the eminent theoretical biologist Aristide Lindenmayer to model the development of dendritic structures in algae. These parallel rewriting systems can emulate how the DNA encodes a program for developing biological organisms. So the L systems, which belong to the mathematical field of formal languages, allow us to write developmental codes or programs that are lexicographically and syntactically correct and for which the encoding can be evolved according to Darwin's law of natural selection. The turtle interpretation acts as translators from the words generated by the L systems into graph topologies. In keeping with our biological analogy, the turtle interpretation emulates the biological processes that compile and execute the genetic information into organism structures. Finally, as in natural systems, the graph topologies generated by the combination of L systems and their turtle interpretations are evolved through a genetic algorithm [23], which uses selection, crossover, and mutation in much the same way as postulated by Darwin's laws and genetic biology. The method is used to determine the solution process for a point-to-area-type heat transfer problem [10–12,24].

## II. Physical Problem

As originally proposed in [10–12,24] in conjunction with constructal theory and recently extended and thoroughly investigated in [13–18], the topology optimization studied here seeks to find the best layout of a highly conducting material of thermal conductivity  $k_f$  distributed over a substrate of thermal conductivity  $k_0$ , where the ratio  $\varepsilon = k_0/k_f \ll 1$ . This optimal layout minimizes the maximum temperature over the physical domain, which is equivalent to the minimization of work lost in a hypothetical heat engine that operates between a finite temperature gap (i.e.,  $T_{\max} - T_0$ ) and it is crossed by a fixed heat current [24]:

$$\dot{S}'_{\text{gen}} = \frac{\dot{Q}'}{T_{\text{max}} T_0} (T_{\text{max}} - T_0) \quad (1)$$

Figure 1 shows the schematics and the notation used in the problem; due to the expected symmetry of the solution, only the upper half, of area  $A/2$ , of the physical domain is simulated. The heat transfer corresponds to pure conduction in an isotropic medium composed of the two previously mentioned materials of thermal conductivity,  $k_f$  and  $k_0$ , in which a constant heat generation of intensity  $q'''$  is applied. The boundary conditions correspond to 1) symmetry condition at the symmetry line and 2) prescribed temperature at a strip of thickness  $\delta_0$  at the lower left corner of the simulation domain and insulation in the remaining part of the boundary (see Fig. 1). At the interface between the distinct materials, heat continuity is applied:

$$k_0 \frac{\partial T}{\partial n} = k_f \frac{\partial T}{\partial n}$$

Having described the optimization problem, in the next section, the topology optimization method used to compute the best layout is described.

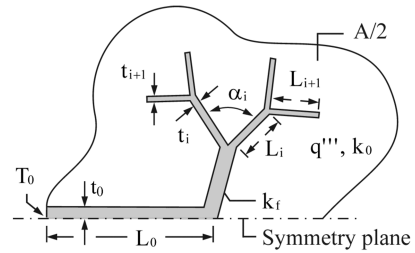


**Fig. 1 Physical domain.**

### III. Bioinspired Optimization Method

The branching topology found in numerous natural systems can be formally modeled as graphs. As mentioned previously, such structures are evolved by using a topology optimization method that combines L systems [19,20] with a turtle interpretation [21,22] as a graph generating grammar. The finite element method is then used for the simulation of each such graph topology and these methods are coupled with a genetic algorithm for the evolution of the optimal dendritic topology modeled by the L systems (see Kobayashi [25] for details about the method).

L systems are parallel rewriting systems consisting of an alphabet  $\Sigma$ , an axiom  $\omega$ , and a finite set of rules  $P$ . The alphabet is a finite nonempty set  $\Sigma$ , for which the elements are called letters. A word  $x$  over  $\Sigma$  is a finite sequence of letters of  $\Sigma$ ; the empty word being denoted by  $\lambda$ . The length of a word  $x$  in  $\Sigma$ ,  $|x|$ , is defined as the number of nonempty letters in  $x$ . The set of all words is denoted as  $\Sigma^*$  and the axiom is a nonempty word. The set of rules in the context-free OL systems considered in the present work can be given as  $a \rightarrow \chi$ , where  $a$  is a letter of the alphabet  $\Sigma$  and  $\chi$  is a word. It is assumed that there is at least one rule for each letter of the alphabet. A OL system is deterministic if for each letter  $a$  in  $\Sigma$ , there is one and only one word  $\chi$  such that  $a \rightarrow \chi$ . Only deterministic L systems are considered in this work and, as a matter of convention, it is assumed that each unspecified rule is the identity rule  $a \rightarrow a$ .

L systems by themselves do not carry any canonical geometric content. So to produce a graph from the words generated by an L system, a translator is needed that associates a graph to each word. In this work, as previously mentioned, the turtle interpretation of the L systems [21,22] is used for the translation. The turtle interpretation operates over general words of  $\Sigma^*$ , and in this regard, it is independent of the L systems. So given a general word  $x$ , in the turtle interpretation, each letter in  $x$  is sequentially read from left to right and interpreted as a command to change the state of the Logo-style turtle. The state of the turtle comprises the turtle position and orientation, given by the Cartesian coordinates of the position of the turtle and the angle  $\theta$  of the head of the turtle with respect to the positive  $x$  axis, together with attributes that changes each branch length and width. Each attribute of the Logo style can change only by a quantum amount identified by the symbol  $\delta$  and a subscript that refers to the attribute; for example,  $\delta_\theta$  refers to the change in the angle  $\theta$  of the turtle head.

Table 1 specifies the set of symbols selected for interpretation in the current work.

The brackets [ and ] function as delimiters of subroutines in the code in that they momentarily deviate the flow of execution of the turtle commands from its current flow to the commands inside the brackets. After the commands inside the bracket are finished, the execution is returned to the first command immediately following the bracket ]. It is this deviation from the current flow that allows these subroutines to produce the branching patterns of the structures. Indeed, a word such as  $A[-A][+A]$  with  $\delta_\theta = 60^\circ$  would first draw a horizontal capped rectangle according to the command  $A$ ; it is assumed that the turtle is initially heading in the positive  $x$ -axis direction. Then the command  $-A$  inside the first bracket would be executed and, accordingly, it would draw a capped rectangle to the left at a  $60^\circ$  angle with the positive  $x$  axis. After drawing this capped rectangle, the turtle would come back to the state at the end of the command that drew the first

**Table 1** Symbols selected for interpretation

Action symbols	Translation
$A, B, \dots$	Cause the turtle to move and draw Move the turtle forward one step and draw a capped rectangle.
$-$	Control the turtle orientation Turn the turtle head to the left by a given increment angle $\delta_\theta$ .
$+$	Turn the turtle head to the right by a given increment angle $\delta_\theta$ .
$[$	Model the branching structure Push the current state of the turtle onto a pushdown stake.
$]$	Pop a state from the stack and make it the current state.

capped rectangle and then execute the command  $+A$ , creating a capped rectangle to the right at a  $-60^\circ$  deg.

In this work, the length and thickness of each branch are also modified when branching. So when branching at a bracket, the capped rectangle is shortened and thinned by quantum ratios  $\delta_1$  and  $\delta_t$ , respectively.

The combination of L systems and their turtle interpretations is best understood with an example. In this example, the L system is defined by the alphabet  $\Sigma = \{A, B, C, [, +, -\}$ , axiom  $\omega = A$ , and production rules

$$A \rightarrow CB, \quad B \rightarrow [+A][-A], \quad C \rightarrow C$$

The parameters controlling the state of the turtle are fixed at  $\delta_\theta = \pi/2$  and  $\delta_t = \sqrt{2}/2$ . The application of the production rules to the axiom generate a new word that is denoted as  $\omega_1$ . Applying the rules to  $\omega_1$  produces  $\omega_2$ , and so on. So the L systems generate a sequence of words  $\{\omega_1, \omega_2, \omega_3, \dots\}$ . Each word in this sequence represents a development stage of the structure, starting from the initial or embryonic stage  $\omega_0$ . Each of these developmental stages can be geometrically interpreted by the turtle interpretation into a developmental structure.

Thus, at the zeroth stage, the word is the axiom  $\omega_0 = A$ . Applying the production rules to the axiom yields the first stage  $\omega_1 = CB$ . Now with two letters, the production rules are simultaneously applied to  $C$  and  $B$ : letter  $B$  is replaced by  $[+A][-A]$  and letter  $C$  is replaced by  $C$  again. The result is  $\omega_2 = C[+A][-A]$ . Repeating this procedure and using the turtle interpretation for each developmental stage produces the following graphs for rounds  $\omega_6$ ,  $\omega_{12}$ , and  $\omega_{18}$  (see Fig. 2). There, it can be seen that the number of bifurcating levels increases with the number of generations and also how the brackets allow for recursive programming (see also [22]).

The search for the optimum dendritic structure is performed using a genetic algorithm (GA) [23]. The genome consists of the production rules, the quantum parameters defining the turtle interpretation, and the parameters defining the shape of the area  $A$ , if applicable. The dimensionless fitness function to be minimized is the maximum dimensionless temperature  $T_{\max}^* = (T_{\max} - T_0)/(q'''A/k_0)$ , which is the same as the one defined in the original work published in [10–12,24]. Because it is expected that the L systems would yield complex dendritic geometries, no general analytical method is available for solving the heat conduction problem. Thus, a numerical solution method was used to solve the following Poisson equation over  $A$ :

$$\nabla^2 T^* + \xi = 0 \quad (2)$$

where  $\xi = 1$  or  $0$  in the heat-generating area and in the highly conductive path, respectively, and  $T^*$  is the dimensionless temperature defined as  $T^* = (T - T_0)/(q'''A/k_0)$  as in [10–12,24].

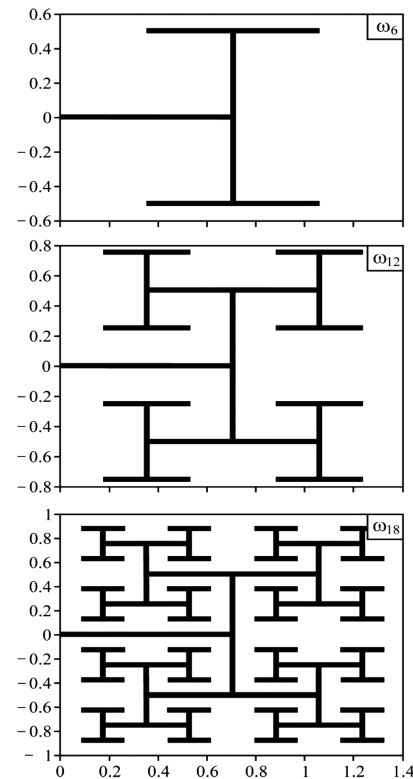
Our numerical simulations were performed using the finite element method (FEM) toolbox COMSOL Multiphysics™, version 3.3, from COMSOL, Inc. [26]. In the next section, we present the validation procedure for simulation results.

#### IV. Validation Procedure

In this section, the validation procedure is described including mesh independence studies and the quantification of convergence of

the solution as the number of degrees of freedom is increased. In all simulations, the quadratic Lagrangian finite element is employed. The quality of the mesh, which is composed of triangles only, can be selected from preassigned mesh sizes or can be manually controlled in COMSOL. In the former mode, there are eight preassigned mesh sizes: extremely coarse, extra coarse, coarser, coarse, normal, fine, finer, and extra fine.

For the validation of the results, several geometries were run before and after the optimization. Next, the results are presented for two representative geometries, one selected from the a priori study and one selected from the a posteriori. The procedure for generating both results is the same. First, a golden solution is obtained with a mesh comprising over half a million degrees of freedom. Then for each of the eight categories of preassigned mesh sizes (extremely coarse, extra coarse, coarser, coarse, normal, fine, finer, and extra fine), the mean mesh size and the relative error for the maximum temperature are determined. The mean mesh size is calculated as the integral of the local mesh size times two; recall that the area of the physical domain is normalized to one and the simulation domain is only half of the physical domain. In this integral, the local mesh size is defined as the length of the largest edge in each triangle of the mesh. To calculate the relative error, the maximum normalized temperature is first calculated for each mesh. With the latter, the relative error for each mesh size is calculated as the absolute value of the difference between the maximum temperature for each mesh and the maximum temperature of the golden solution, divided by the maximum temperature of the golden solution.

**Fig. 2** Turtle interpretation: rounds  $\omega_6$ ,  $\omega_{12}$ , and  $\omega_{18}$ .

For the a priori validation, Fig. 3 shows the variation of the relative error as a function of the mean mesh size [normalized by the mean mesh size ( $h = 0.02633705$ ) of the extremely coarse mesh] for each of the preceding eight mesh categories and for a typical complex topology. Also shown in the figure is the combination of the golden solution (upper half) and the mesh corresponding to the normal mesh (lower half). Such irregular geometry constitutes a difficult problem for the automatic mesh generation algorithm. The results clearly indicate the adequacy of all meshes, as all errors are smaller than 0.2% of the golden solution. In particular, the normal and fine results are almost indistinguishable. Based on the fact that the normal mesh results in reasonable mesh sizes and produce accurate solutions, it was decided to use the normal size for the simulation of each individual in the optimization procedure.

The preceding results represent the studies performed a priori. After the optimization, the best individuals are validated again to confirm the reliability of the results. Figure 4 shows the variation of the relative error as a function of the mean mesh size, again normalized by the mean mesh size ( $h = 0.0296195$ ) of the extremely coarse mesh, for each of the preceding eight mesh categories, but now for the overall optimal design. As in Fig. 3, also shown in the figure are the golden solution and the mesh corresponding to the

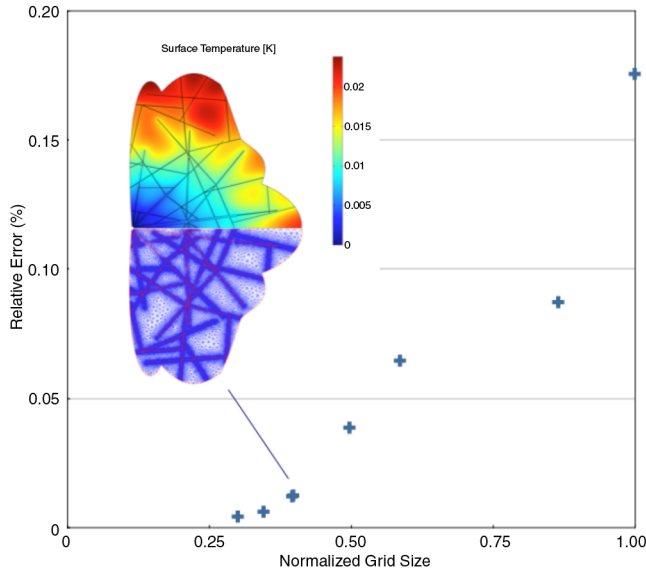


Fig. 3 Validation a priori.

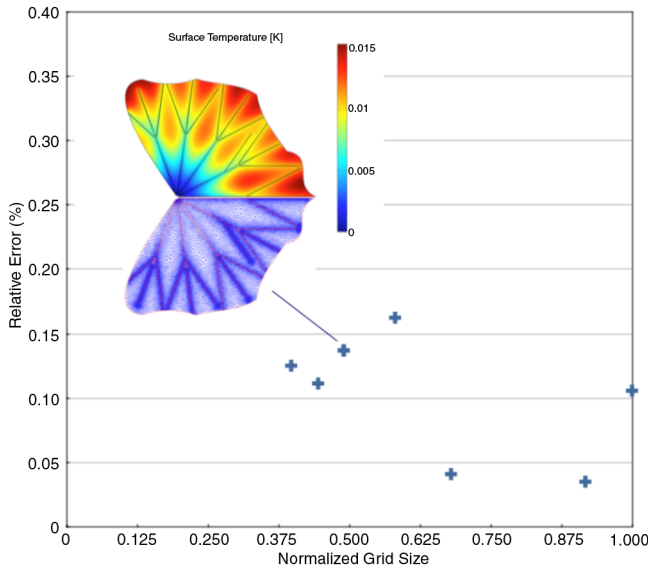


Fig. 4 Validation a posteriori.

normal mesh. These results confirm the adequacy of the normal mesh for computing the figure of merit of each individual and also validate the results obtained with the proposed bioinspired methodology.

## V. Results and Analysis

The evolution of the designs used two genetic operators: crossover and mutation [27]. The crossover acts on 80% of the population, with parental selection based on the stochastic uniform method; the gene recombination is performed with the scattered method. A Gaussian mutation with shrinking variance was selected for the mutation operator.

In the GA, an initial population of 100 individuals ( $n_{\text{ind}}$ ) was used. The population was allowed to evolve for a minimum of 200 generations ( $n_{\text{gen}}$ ). Every additional round of application of the production rules can generate more complex topologies.

As a first optimization problem, a fixed square shape is imposed for the heat-generating area ( $A = L \times L$ ) and to study the effect of the number of production rules applied to the evolutionary process on our figure of merit. In the simplest topology, called elemental [10–12,24], no bifurcation is allowed and the fin is a rectangle of length  $L$  and thickness  $t_0 = A(\Phi_f/L)$  dividing the area  $A$  through the symmetry plane ( $i = 0$ ). The performance of this configuration, which was used as a benchmark, yields a fitness function of  $T_{\text{max},0}^*|_{\text{min}} = 0.482551$ . Figure 5 shows the effect of the optimized complexity on the normalized fitness function for structures of higher complexity. As the complexity of the dendritic structure increases, a substantial improvement of the value of the normalized fitness function occurs, which agrees with previous studies [7,10–12,24]. Our results show that when the production rules are applied only once ( $i = 1$ ), the normalized fitness function of the fittest individual drops roughly by 50% of its original value. Further improvements are obtained as more rounds of production rules are applied. For each

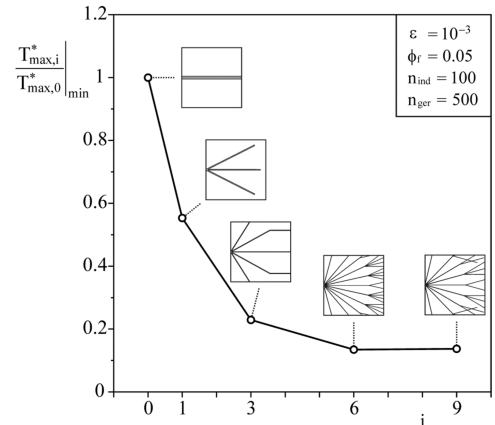


Fig. 5 Effect of the number of production rules on the fittest individuals.

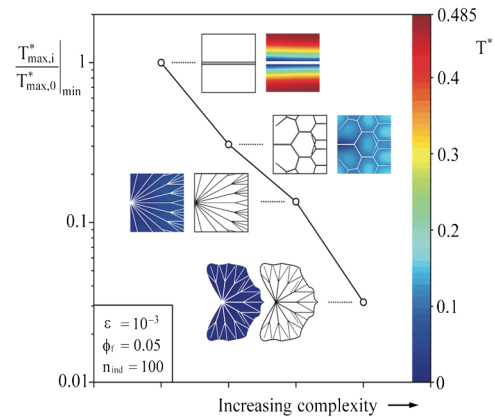


Fig. 6 Effect of the optimized complexity on the fitness function.



value of  $i$  shown in Fig. 5 (open symbols), which present the fittest individual for that given number of production rounds, it is possible to identify an optimum level of complexity, defined here as the number and variety of bifurcations [10–12,24], in which reductions of the normalized fitness function are almost on the order of 90% of its original value (i.e.,  $i = 6$  and 9). Moreover, one should note that the complexity of the topology of the dendritic structure increased between  $0 \leq i \leq 6$ . For  $i > 6$ , the dendritic topology reaches a stable level, because the optimized topology obtained for  $i = 6$  and 9 are similar in terms of bifurcations levels. This means that the evolutionary process does not add more bifurcations to the structure in which  $i = 9$ , because this would not reduce the normalized fitness function. This agrees with previous observations made with constructal theory [7,10–12,24]. Obviously, the optimal number of bifurcations is a highly dependent function of  $\varepsilon$  and  $\Phi_f$ . Similar dendritic trees were obtained in [7] for fluid-draining networks.

The allowed complexity of the design is a function of the number of rounds of application of the production rules and of the shape of the heat-generating area. For instance, in Fig. 6 the shape is defined by five polar cubic Bezier curves. In Fig. 6 the effect of complexity on the normalized figure of merit is studied. Four different complexity levels are considered: from left to right, the abscissa shows the elemental design; the optimum design obtained with the L system shown in [8], which was optimized for the quantum parameters  $\delta_\theta$ ,  $\delta_l$ , and  $\delta_r$ ; the third design, which allows any type of topology for the dendritic structure (see Fig. 5); and finally, the combined shape and topology design. The variation of the normalized figure of merit with complexity clearly indicates the beneficial effect of complexity in the design, in which the figure of merit changes by nearly 2 orders of magnitude from the elemental design (upper left corner) to the highly efficient free-shape design presented on the lower right corner. Similar results were obtained by previous studies [7,8,10–12]. The four dual frames for each complexity level show not only the topology of the fittest individual for that complexity level, but also the effect of the topology on the temperature distribution over A.

In Fig. 7 the efficiency of complex low-entropy systems is analyzed by comparing the combined frequency of 200 viable individuals with two different levels of complexity. Indeed, because the proposed optimization method uses the genetic algorithm, the figures of merit for each individual of each generation and for all generations are readily available in the end of the optimization process. So it is possible to explore the robustness of the complex design by constructing the histogram of the frequency of individuals for which the figure of merit lay in preassigned ranges of the latter. Thus, with the available individuals, the evolving designs were accounted for at two different stages of the evolutionary process (i.e., initial generation  $IG = 1$  and at the generation number 20,  $IG = 20$ ). The reason for selecting  $IG = 1$  and 20 stems from the fact that for

$IG = 1$ , all individuals are randomly generated and nonoptimized. For  $IG = 20$ , the individuals were somewhat evolved, but not necessarily all converged, at least to complex systems, which offers a chance for further evolution of the population. The evolved structures for each complexity level considered in Fig. 7 are shown in Fig. 6 (second and fourth frames). The open symbols located in the abscissa of each frame refer to the minimal value of merit function obtained for the converged design, which was shown previously in Fig. 6 for honeycomblike and free-shape designs. Two main observations can be made based on Fig. 7. First, there is rapid convergence observed for low-complexity systems, because both upper frames present a highly converged population of viable individuals, even for  $IG = 1$ . As for the lower frames, a much larger diversity of individuals is observed. Second, and more important, the rapid convergence of simple systems does not necessarily translate into high-performing, low-entropy, heat-generating systems. In other words, highly complex systems can easily outperform simpler designs even at a nonoptimized stage, which is confirmed by observing the abscissa of the upper and lower frames plotted for the same scale. Together, both observations support complexity as a robust feature of low-entropy thermal systems, which is in agreement with previous studies [7,10–12,24] based on constructal theory.

## VI. Conclusions

In closing, the present work demonstrates the feasibility and efficiency of coupling the L system and a FEM through a GA to discover unbiased or preassumed dendritic topologies while minimizing the entropy of thermal systems. Additionally, the combined L system and GA optimization approach described in this work explicitly shows that complexity can be generated in a genetic basis and according to the evolution laws of natural selection and that the added complexity thus created can be an asset in the generation of low-entropy thermal systems as previously shown [7,10–12,24]. This is an important finding because it quantifies the robustness of the evolved structure to the inherently stochastic fluctuations in the genotypic mutation and natural selection conditions affecting the evolution process of these structures [7,10–12,24].

## Acknowledgment

The authors are grateful for the partial support by U.S. Air Force Office of Scientific Research grant FA9550-07-01-0036.

## References

- [1] Lotka, A. J., "Contribution to the Energetics of Evolution," *Proceedings of the National Academy of Sciences*, Vol. 8, No. 6, 1922, pp. 147–151.
- [2] Thompson, D. W., "On Form and Mechanical Efficiency," *On Growth and Form*, 2nd ed., Cambridge Univ. Press, Cambridge, England, U.K., 1942, pp. 221–267.
- [3] Vogel, S., "More About Circulatory Systems," *Comparative Biomechanics: Life's Physical World*, Princeton Univ. Press, Princeton, NJ, 2003, pp. 205–225.
- [4] Carroll, S. B., "Chance and Necessity: the Evolution of Morphological Complexity and Diversity," *Nature*, Vol. 409, Feb. 2001, pp. 1102–1109. doi:10.1038/35059227
- [5] Odum, H. T., "Emergy and Real Wealth," *Environmental Accounting: Energy and Decision Making*, Wiley, New York, 1996, pp. 1–14.
- [6] Rosen, R., "Life Itself: The Preliminary Steps," *Life Itself: A Comprehensive Inquiry Into the Nature, Origin and Fabrication of Life*, Columbia University Press, New York, 1991, pp. 244–253.
- [7] Bejan, A., "Natural Form, Questioning, and Theory," *Shape and Structure, from Engineering to Nature*, Cambridge Univ. Press, Cambridge, England, U.K., 2000, pp. 1–13.
- [8] Pedro, H. T. C., Kobayashi, M. H., Coimbra, C. F. M., and da Silva, A. K., "Effectiveness of Complex Design Through an Evolutionary Approach," *Journal of Thermophysics and Heat Transfer*, Vol. 22, No. 1, 2008, pp. 115–118. doi:10.2514/1.29834
- [9] Schneider, E., and Sagan, D., "Nature Abhors a Gradient," *Into the Cool-Energy Flow, Thermodynamics, and Life*, Univ. of Chicago Press, Chicago, 2005, pp. 72–77.

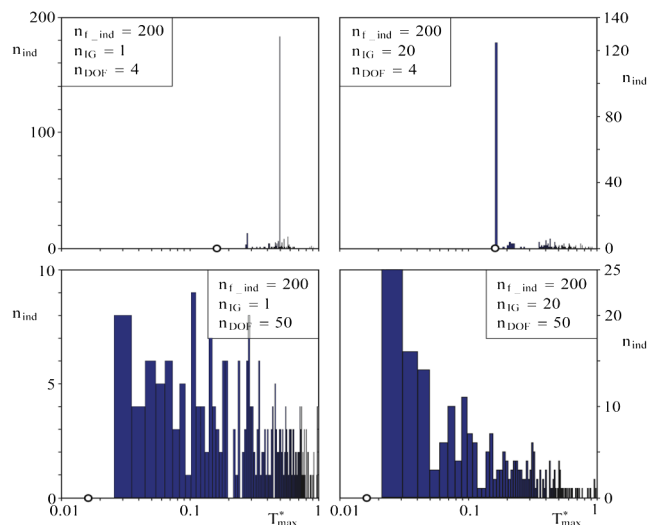


Fig. 7 Robustness and diversity of complexity on the entropy generation.

- [10] Bejan, A., "Constructal-Theory Network of Conducting Paths for Cooling a Heat Generating Volume," *International Journal of Heat and Mass Transfer*, Vol. 40, No. 4, 1997, pp. 799–816.  
doi:10.1016/0017-9310(96)00175-5
- [11] Ledezma, G. A., Bejan, A., and Errera, M. R., "Constructal Tree Networks for Heat Transfer," *Journal of Applied Physics*, Vol. 82, No. 1, 1997, pp. 89–100.  
doi:10.1063/1.365853
- [12] Errera, M. R., and Bejan, A., "Deterministic Tree Networks for River Drainage Basins," *Fractals*, Vol. 6, No. 3, 1998, pp. 245–261.  
doi:10.1142/S0218348X98000298
- [13] Li, Q., Steven, G. P., Querin, O. M., and Xie, Y. M., "Shape and Topology Design for Heat Conduction by Evolutionary Structural Optimization," *International Journal of Heat and Mass Transfer*, Vol. 42, No. 17, 1999, pp. 3361–3371.  
doi:10.1016/S0017-9310(99)00008-3
- [14] Li, Q., Steven, G. P., Xie, Y. M., and Querin, O. M., "Evolutionary Topology Optimization for Temperature Reduction of Heat Conducting Fields," *International Journal of Heat and Mass Transfer*, Vol. 47, No. 23, 2004, pp. 5071–5083.  
doi:10.1016/j.ijheatmasstransfer.2004.06.010
- [15] Bendsøe, M. P., and Sigmund, O., "Extensions and Applications," *Topology Optimization—Theory, Methods, and Applications*, Springer, New York, 2004, pp. 71–158.
- [16] Gersborg-Hansen, A., Bendsøe, M. P., and Sigmund, O., "Topology Optimization of Heat Conduction Problems Using the Finite Volume Method," *Structural and Multidisciplinary Optimization*, Vol. 31, No. 4, 2006, pp. 251–259.  
doi:10.1007/s00158-005-0584-3
- [17] Mathieu-Potvin, F., and Gosselin, L., "Optimal Conduction Pathways for Cooling a Heat-Generating Body: A Comparison Exercise," *International Journal of Heat and Mass Transfer*, Vol. 50, Nos. 15–16, 2007, pp. 2996–3006.  
doi:10.1016/j.ijheatmasstransfer.2006.12.020
- [18] Bruns, T. E., "Topology Optimization of Convection-Dominated, Steady-State Heat Transfer Problems," *International Journal of Heat and Mass Transfer*, Vol. 50, Nos. 15–16, 2007, pp. 2859–2873.  
doi:10.1016/j.ijheatmasstransfer.2007.01.039
- [19] Lindenmayer, A., "Mathematical Models for Cellular Interaction in Development—Part 1," *Journal of Theoretical Biology*, Vol. 18, No. 3, 1968, pp. 280–299.  
doi:10.1016/0022-5193(68)90079-9
- [20] Lindenmayer, A., "Mathematical Models for Cellular Interaction in Development—Part 2," *Journal of Theoretical Biology*, Vol. 18, No. 3, 1968, pp. 300–315.  
doi:10.1016/0022-5193(68)90080-5
- [21] Abelson, H., and DiSessa, A. A., "Introduction to Turtle Geometry," *Turtle Geometry: The Computer as a Medium for Exploring Mathematics*, Massachusetts Inst. of Technology Press, Cambridge, MA, 1981, pp. 3–54.
- [22] Prusinkiewicz, P., and Lindenmayer, A., "Graphical Modeling Using L-Systems," *The Algorithmic Beauty of Plants*, Springer, New York, 2004, pp. 1–50.
- [23] Holland, J., "Genetic Algorithms and the Optimal Allocations of Trials," *SIAM Journal on Computing*, Vol. 2, No. 2, 1973, pp. 88–105.  
doi:10.1137/0202009
- [24] Bejan, A., "The Two Laws Combined: the Destruction of Exergy," *Advanced Engineering Thermodynamics*, 2nd ed., Wiley, New York, 1997, pp. 108–150.
- [25] Kobayashi, M. K., "On a Biologically Inspired Topology Optimization Method," *Communications in Nonlinear Science and Numerical Simulation* (to be published).  
doi:10.1016/j.cnsns.2009.04.014
- [26] COMSOL Multiphysics, Software Package, Ver. 3.3, COMSOL, Inc., Burlington, MA, Aug. 2006.
- [27] Goldberg, D., "Computer Implementation of a Genetic Algorithm," *Genetic Algorithms in Search, Optimization and Machine Learning*, Addison-Wesley, Reading, MA, 1989, pp. 59–88.